Polaron excitations in doped C_{60}: Effects of disorder

Kikuo Harigaya*
Department of Physics, University of Sheffield, Sheffield S3 7RH, United Kingdom
and Fundamental Physics Section, Physical Science Division, Electrotechnical Laboratory,
Umezono 1-1-4, Tsukuba, Ibaraki 305, Japan†
(Received 12 March 1993)

The effects on C_{60} of thermal fluctuations of phonons, misalignment of C_{60} molecules in a crystal, and other intercalated impurities (C_{70}, oxygens, and so on) are simulated by disorder potentials. The Su-Schrieffer-Heeger–type electron-phonon model for doped C_{60} is solved with Gaussian bond disorder and also with site disorder. Sample averaging is performed over a large number of disorder configurations. The distribution of bond lengths and electron densities are shown as functions of the disorder strength and the additional electron number. The stability of polaron excitations as well as dimerization patterns are studied. Polarons and dimerization in lightly doped cases ($C_{60}^{-1,-2}$) are relatively stable against disorder, as is indicated by peak structures in the distribution functions. In more heavily doped cases, several peaks merge into a single peak, showing the breakdown of polaron structures as well as the decrease of the dimerization strength. The possibility of observation of polaronic lattice distortions and electron structures in doped C_{60} is discussed.

I. INTRODUCTION

Recently, the fullerenes C_N which have a hollow cage structure of carbons have been intensively investigated. There are several experimental indications that the doped fullerenes show polaronic properties due to the Jahn-Teller distortion, for example: (1) The electron-spin-resonance (ESR) study[1] on the radical anion of C_{60} has revealed the small g factor, $g=1.9991$, and this is associated with the residual orbital angular momentum due to the Jahn-Teller distortion. (2) Photoemission studies[2] of C_{60} and C_{70} doped with alkali metals have shown peak structures, which cannot be described by a simple band-filling picture. (3) When poly(3-alkylthiophene) is doped with C_{60},[3] interband absorption of the polymer is greatly suppressed and the new absorption peak evolves in the low-energy range. The Jahn-Teller splitting of the lowest unoccupied molecular orbital (LUMO) in the C_{60}^- state and/or the Coulomb attraction of a positively charged polaron to C_{60}^- might occur. (4) The luminescence of neutral C_{60} has been measured.[4] There are two peaks around 1.5 and 1.7 eV below the gap energy 1.9 eV, interpreted by the effect of the polaron exciton. In addition, the experiments on the dynamics of photoexcited states have shown the interesting roles of polarons.[5]

Several authors[6,7] have proposed an interacting electron-phonon model in order to describe the polarons in doped C_{60}. The Su-Schrieffer-Heeger (SSH) model of conjugated polymers[8] has been extended to fullerenes in these works.[6,7] The π electrons hop between nearest-neighbor sites. The hopping integral depends linearly on the change of the bond length. The bond modeled by the classical harmonic spring is the contribution from the σ bonding. In the previous paper,[9] we have calculated lattice distortion and electronic structures of the molecules, where one to six electrons are added, or one to ten electrons are removed. When C_{60} is doped with one or two electrons (or holes) (the lightly doped case), the additional charges accumulate at 20 carbon atoms along almost an equatorial line of the molecule. The dimerization becomes the weakest along the same line. Two energy levels, the occupied state and the empty state, intrude largely in the gap. These are the polaron effects. The changes of the electronic structure of the molecules with more charges (the heavily doped case) have been reported in Ref. 9. However, the complex changes of lattice geometries and electron-density distributions have not shown yet. Section III of this paper will be devoted to this purpose.

In the study in Ref. 9, the molecule has been assumed to be isolated and the calculations have been done within the adiabatic approximation. However, it has been discussed[10] that the width of the zero-point motion in conjugated polymers and fullerene tubules is of the order of 0.01 Å. The same order of magnitude would be expected in C_{60}.[11] This is also of the same order as the difference between the short and long bond lengths: 0.05 Å.[12] Therefore, the polaronic distortion described in the adiabatic approximation might change its structures by thermal fluctuations. The thermal fluctuation effects can be simulated by introducing the bond disorder potentials. The doped SSH system with Gaussian bond disorders will be studied in Sec. IV.

It is known that C_{60} molecules contain a small amount of C_{70} as impurities.[4] Sometimes the C_{60} films and solids are contaminated with oxygen.[4,13] Misalignment of molecules in C_{60} solids would remain. These effects would be good origins of additional potentials acting on π electrons at the carbon sites. They can be modeled by random site disorder. Site disorder effects will be investigated in Sec. V.

A sample average is performed over a large number of independent disorder configurations. The distribution functions of bond lengths and electron densities are cal-

0163-1829/93/48(4)/2765(8)/$06.00

culated with changes to the disorder strength and the additional electron number. We mainly consider stability of polaron excitations as well as dimerization patterns. We find that polarons and dimerizations in lightly doped cases are rather stable against disorder. This property is common to bond and site disorder effects. In more heavily doped cases, the several peaks in distribution functions merge into a single peak. This indicates that polaron structures are broken while the dimerization strength decreases, owing to doped charges and disorder.

This paper is organized as follows. We explain the model in the next section. In Sec. III, the lattice and electronic patterns of electron-doped C_{60} are extensively reported. In Sec. IV, bond disorder effects are studied. Section V is devoted to site disorder effects. We close this paper with a summary and a discussion in Sec. VI.

II. MODEL

The extended SSH Hamiltonian for the fullerene C_{60},[9]

$$H_{\rm SSH}=\sum_{\langle i,j\rangle,\sigma}(-t_0+\alpha y_{i,j})(c_{i,\sigma}^{\dagger}c_{j,\sigma}+\text{H.c.})+\frac{K}{2}\sum_{\langle i,j\rangle}y_{i,j}^2 , \tag{1}$$

is studied with Gaussian bond disorder,

$$H_{\rm bond}=\alpha\sum_{\langle i,j\rangle,\sigma}\delta y_{i,j}(c_{i,\sigma}^{\dagger}c_{j,\sigma}+\text{H.c.}) , \tag{2}$$

as well as with Gaussian site disorder,

$$H_{\rm site}=\sum_{i,\sigma}U_i c_{i,\sigma}^{\dagger}c_{i,\sigma} . \tag{3}$$

In $H_{\rm SSH}$, $c_{i,\sigma}$ is an annihilation operator of a π electron; the quantity t_0 is the hopping integral of the ideal undimerized system; α is the electron-phonon coupling; $y_{i,j}$ indicates the bond variable which measures the change of the length of the bond between the ith and jth sites from that of the undimerized system; the sum is taken over nearest-neighbor pairs $\langle i,j\rangle$; the second term is the elastic energy of the lattice; and the quantity K is the spring constant. The part $H_{\rm bond}$ is the disorder potential due to the Gaussian modulation of transfer integrals. The disorder strength is measured by the standard deviation y_s of the bond variable modulations $\delta y_{i,j}$. The mean value of $\delta y_{i,j}$ is assumed to be zero. The term $H_{\rm site}$ is the site disorder potential. The quantity U_i is the strength of the disorder at the ith site, with the standard deviation U_s. The model is solved with the assumption of the adiabatic approximation and by an iteration method used in Ref. 9.

III. POLARONS IN C_{60}

In this section, we present a detailed discussion on the polarons of the electron-doped C_{60}. Further data concerning the lattice and electron-density structures are reported. In Ref. 9, only the electronic energy levels and averaged dimerization strengths were discussed for heavily doped C_{60}.

In Fig. 1, the unfolded figure of the truncated icosahedron is shown. When we make the paper model of C_{60}, we cut the figure along the outer edges of white hexagons. After folding edges between neighboring hexagons and combining several edges, we obtain a closed structure of the molecule. The shadowed hexagons in Fig. 1 become pentagons. The symbols $A-L$ specify different pentagons.

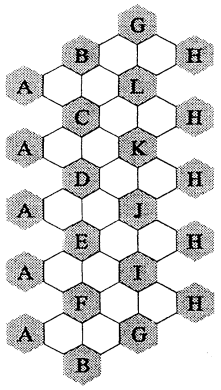

FIG. 1. Unfolded pattern of the paper model of C_{60}. See the text for the notations.

The model equation (1) is numerically solved for the parameters: $t_0=2.1$ eV, $\alpha=6.0$ eV/Å, and $K=52.5$ eV/Å^2. These give the characteristic scales for the neutral C_{60}: the total π-band width $6t_0=12.6$ eV, the energy gap 1.904 eV, and the difference of the bond length between the short and long bonds 0.4557 Å. These values are typical. They are slightly different from those in Ref. 9, but the qualitative features of solutions are not affected by the slight modifications. Quantitative differences are small, too. The total electron number is changed within $N\le N_{\rm el}\le N+6, N=60$ being the number of sites.

In Fig. 2, the magnitudes of bond variables are shown in the upper figures by changing the electron number. The bond is represented by a bold line when it is shorter and $y_{i,j}<0$. The bond is represented by a dashed line when it is longer and $y_{i,j}>0$. The thickness of the line indicates $|y_{i,j}|$. The valence number (the negative of the additional electron number) of the doped molecule accompanies each figure. The lower figures show the additional electron density. The area in each circle is proportional to the absolute value.

In $C_{60}^{1-,2-}$, most (about 70–80 %) of the additional charges accumulate at 20 carbon atoms along an equatorial line of the molecule. At the same time, the difference between the lengths of the short and long bonds becomes smallest at sites along the same equatorial line. This means that the dimerization strength is weakest. Two nondegenerate energy levels intrude largely in the energy gap as shown in Fig. 2(a) of Ref. 9. These lattie and electronic structures are the same as those of polarons in conjugated polymers, so we named the changes polaron excitations. A fivefold axis penetrates between the centers of the pentagons, A and H.

When C_{60} is doped with three electrons, the symmetry is highly reduced. There is only an inversion symmetry. Only two sites have the same electron density. Only two

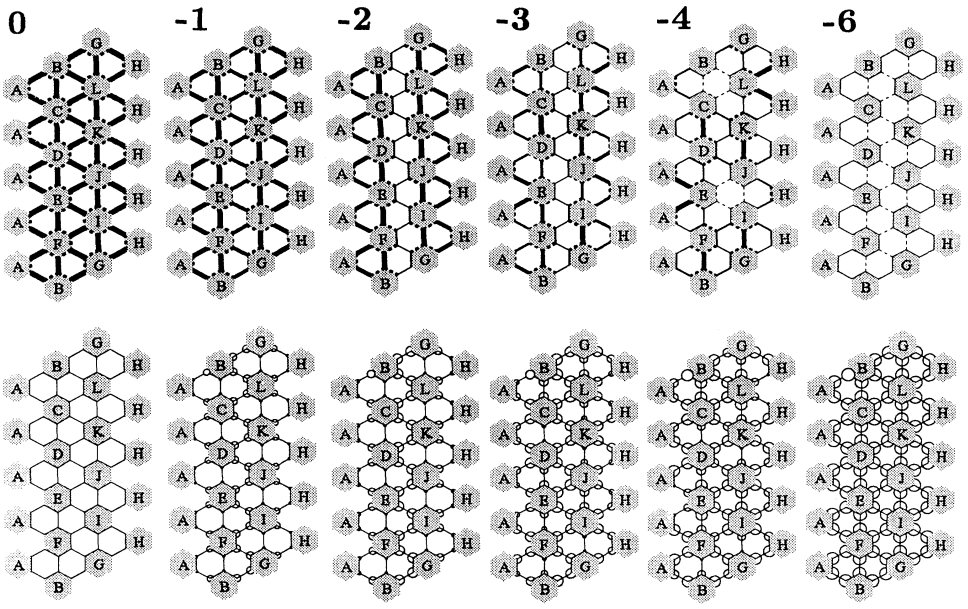

FIG. 2. Bond variables and excess electron densities shown on the unfolded pattern of doped C_{60} without disorders. The upper figures show the bond variables, while lower figures display excess electron densities. The number at the top is $N-N_{\rm el}$. Notations are explained in the text.

bonds have the same length. As shown in Fig. 2, additional electron densities have large values at the 20 carbon atoms along the equatorial line as well as at the other sites near the pentagons, A and H. The energy levels are shown in Ref. 9. The 31st wave function has large amplitudes at sites along the equatorial line, while the 32nd one has larger amplitudes at the other sites. The distribution of the electron density reflects this property.

When the molecule is further doped and the additional electron number is 4, the dimerization pattern changes qualitatively. The symmetry becomes higher and there is a threefold axis which penetrates the center of the hexagon surrounded by the pentagons, B, C, and L. The molecule doped with five electrons has the similar bond alternation pattern and the same symmetry (the figures are not shown for the simplicity). Finally, in the molecule doped with six electrons, the dimerization almost disappears and is rather negligible. The icosahedral symmetry is recovered.

IV. BOND-DISORDER EFFECTS

The SSH model $H_{\rm SSH}$ is solved with the bond disorders $H_{\rm bond}$. The additional electron number, $n \equiv N_{\rm el}-N$, is changed within $0 \le n \le 6$. The most realistic origin for bond disorders is the thermal fluctuation of phonons. So, we shall change the strength of the disorder in the range comparable with that of the amplitude of thermal fluctuations. It has been discussed[10] that the width of the zero-point motion of phonons is 0.03–0.05 Å in conjugated polymers and is of the same order in fullerenes. So, it is reasonable to assume that the maximum value of y_s is of the similar magnitude. We take $y_s=0.01$, 0.03, and 0.05 Å.

A fairly large number of mutually independent samples of disorders are generated, and the model, Eqs. (1) and (2), is solved for each sample. The bond variable and electron density are counted in order to draw histograms of distributions. The sample number 5000 yields a good convergence.

Figure 3 shows the distributions of bond variable $D(y)$. The thick, thin, and dashed lines are for $y_s=0.01$, 0.03, and 0.05 Å, respectively. The ordinate is normalized so that the area between the curve and the abscissa is unity. Figure 3(a) for neutral C_{60} shows the two-peak structure, related to the presence of the dimerization: the positive $y_{i,j}$ corresponds to the longer bond, while the negative one corresponds to the short bond. The magnitude of the zero-point motion would be of the order 0.01 Å. For example, the treatment of the H_g-type phonon within the framework of the SSH model by Friedman and Harigaya has resulted in the magnitude being about 0.01–0.02 Å as the adiabatic energy curve in Ref. 11 indicates. The curve of $y_s=0.01$ Å has two peaks which are clearly separated. The curve of $y_s=0.03$ Å still shows distinct peaks. Therefore, the dimerization survives thermal fluctuations in the neutral molecule. Actually, the nuclear magnetic resonance[12] (NMR) shows the existence of the dimerization. When doped further up to $C_{60}{}^{1-,2-}$, the dimerization seems to remain against disorder: the two peaks can be identified. However, another peak emerges between the two peaks for $y_s=0.01$ Å when doped with two electrons. This peak corresponds to the small bond variables which have been located along the equatorial line in the impurity-free case. Thus, the polaronic distortion seems to persist, too.

Figure 4 shows the distributions of the electron density per site $D(\rho)$. In ρ, the electron density of the impurity-free half-filled system is subtracted. The notations of the lines are the same as in Fig. 3. Figure 4(a) shows the nearly uniform electron density. When doped with one or two electrons, a shoulder develops at the positive-ρ side of the curve. This is owing to the accumulation of the extra charge in the limited carbon sites of the molecule as found in Fig. 2. The dimerization begins to be broken in the same portion. And also, the central peak

around $\rho=0$ still remains, due to the smaller changes of the electron density at sites of the pentagons, A and H, of Fig. 2. Thus, the polaronic charge distribution persists in the presence of bond disorders.

Next, we discuss heavily doped cases with $n \geq 3$. In the distribution function of the bond variables, the three peaks merge into a single peak centered around $y=0$ Å. This is owing to the dimerization, the strength of which became very smaller. The polaronic distortion becomes smaller also, as indicated by the averaged dimerization $\langle |y_{i,j}| \rangle$ presented in Table III of Ref. 9. The electron distribution functions shown in Figs. 4(d) and 4(e) have a

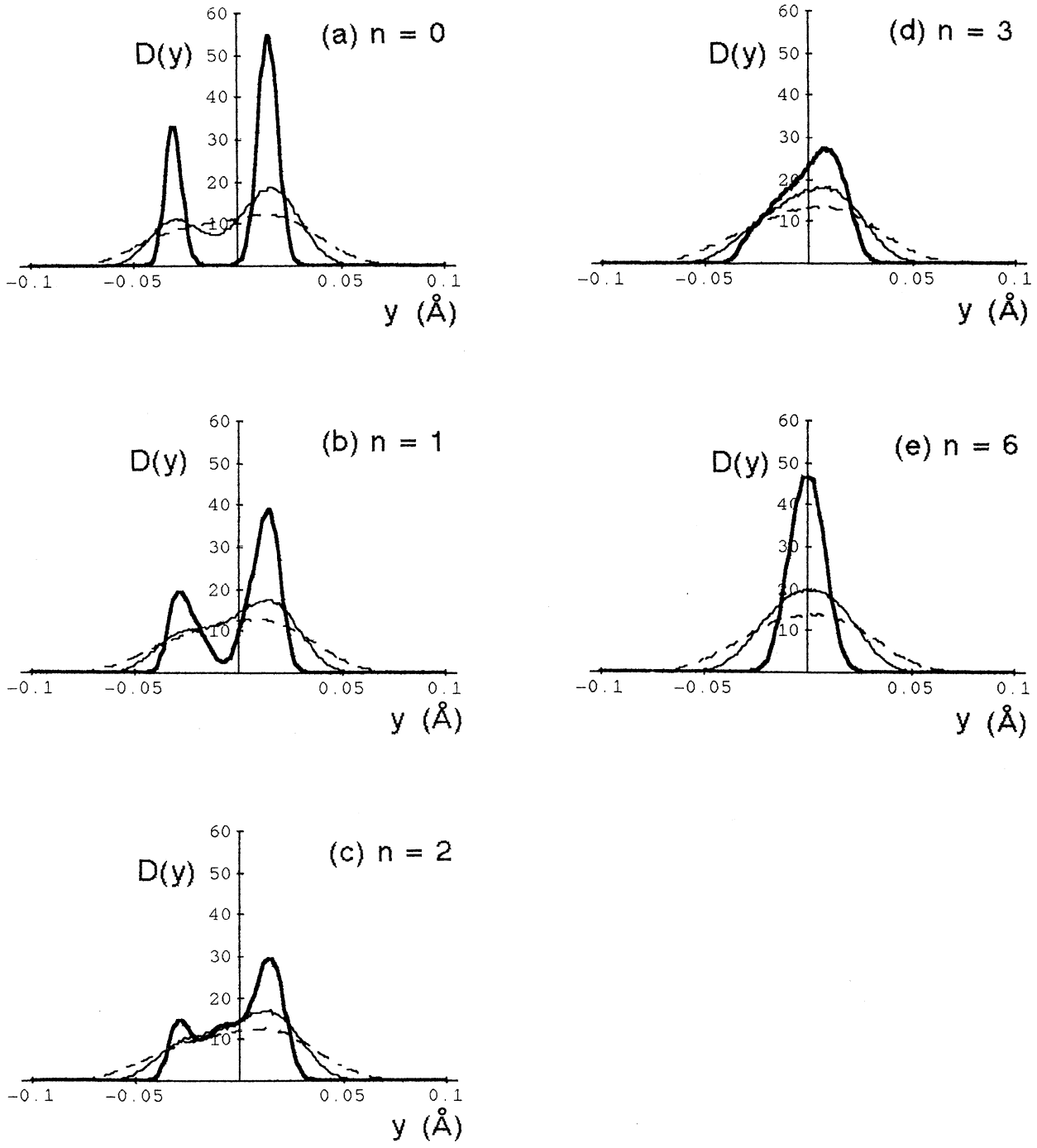

FIG. 3. Distribution function $D(y)$ of bond variables y of the doped C_{60} in the presence of bond disorders. The ordinate is normalized so that the area between the curve and the abscissa is unity. The thick, thin, and dashed lines are for $y_s=0.01$, 0.03, and 0.05 Å, respectively.

largest peak centering the value n/N which is the result of the uniform doping. This is also related to the breakdown of the bond alternation pattern.

V. SITE-DISORDER EFFECTS

The model equations (1) and (3) are solved for each sample of site disorder potentials. Taking the number of samples up to 5000 yields a nice convergence of the distribution functions. We assume three values for disorder strength: $U_s=0.5$, 1.0, and 2.0 eV. The calculation of the Madelung potential in the solid C_{60} (Ref. 14) has yielded the variation of the potential on the surface of C_{60} within 0.5 eV. Therefore, the misalignment of C_{60} in the solid gives rise to the similar strength of site disorder. The other intercalated impurities (C_{70},[4] oxygens,[4,13]

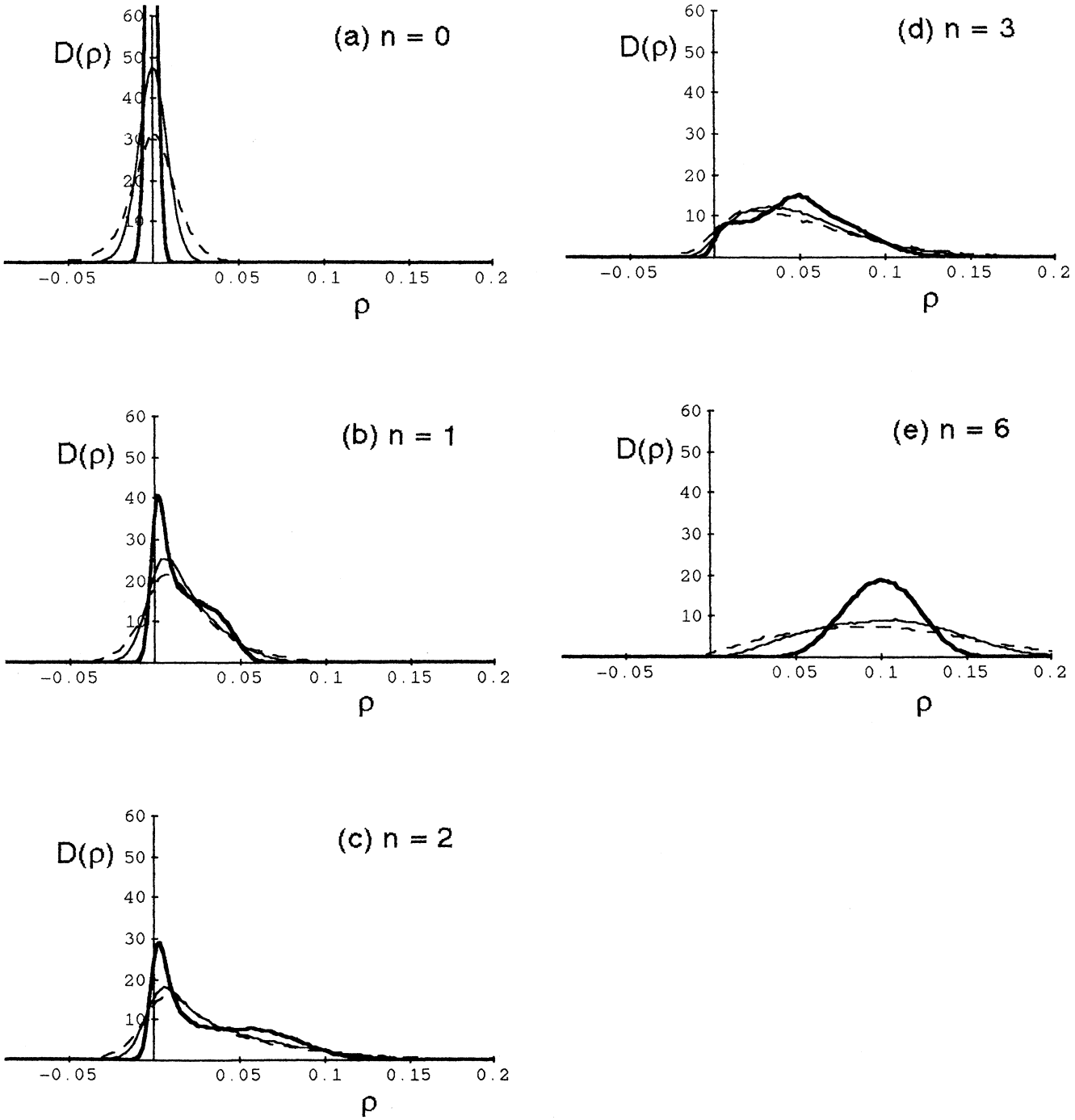

FIG. 4. Distribution function $D(\rho)$ of the excess electron density of the doped C_{60} in the presence of bond disorders. The ordinate is normalized so that the area between the curve and the abscissa is unity. The thick, thin, and dashed lines are for $y_s=0.01$, 0.03, and 0.05 Å, respectively. ρ is measued in units of excess electron density.

dopants,[2] and so on) might yield site disorder potentials of the order of 1 eV. These are the realistic origins of site disorders. The additional electron number n is changed up to 6.

Figure 5 shows the distribution functions of bond variables $D(y)$. The thick, thin, and dashed lines are for $U_s=0.5$, 1.0, and 2.0 eV, respectively. While the molecule is weakly doped ($n=1,2$), the dimerization tends to survive disorder potentials. This is easily seen by thick and thin lines in Figs. 5(b) and 5(c). The dashed lines have a single peak. This is due to the strong disorder potential comparable to the size of the energy gap of the undoped molecule; the dimerization becomes undiscernible, when energies of the occupied and unoccupied electronic

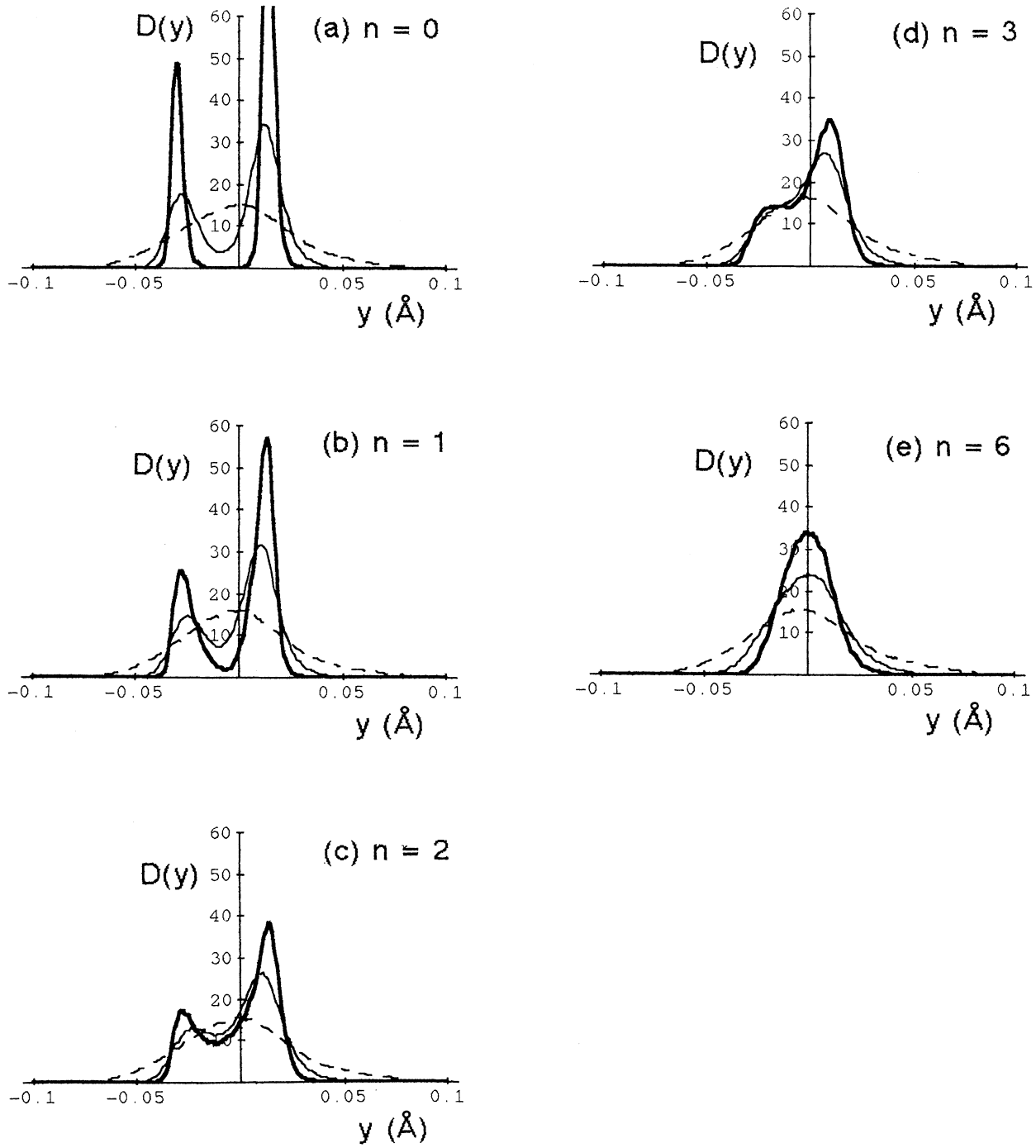

FIG. 5. Distribution function $D(y)$ of bond variables y of the doped C_{60} in the presence of site disorders. The ordinate is normalized so that the area between the curve and the abscissa is unity. The thick, thin, and dashed lines are for $U_s=0.5$, 1.0, and 2.0 eV, respectively.

states are closer. The actual site potentials would not be so strong as that of the dashed line, in view of the screening effects due to the π electrons spread over the surface of the molecule. Therefore, the dimerization persists strongly when site disorders are present.

When the doping proceeds further ($3 \leq n \leq 6$), the two major peaks join into a single peak in $D(y)$. This shows that the dimerization is easy to disappear due to the disorder potentials as well as the densely accumulated extra charges.

Figure 6 shows charge-density distributions $D(\rho)$. We show results only for $n=0$, 3, and 6, because the qualitative features are the same for all n. The notations are the same as in Fig. 5. The charge density is directly modulated by the site disorder. So, each curve has the shape near the Gaussian distribution. The value of ρ at the peak is close to n/N.

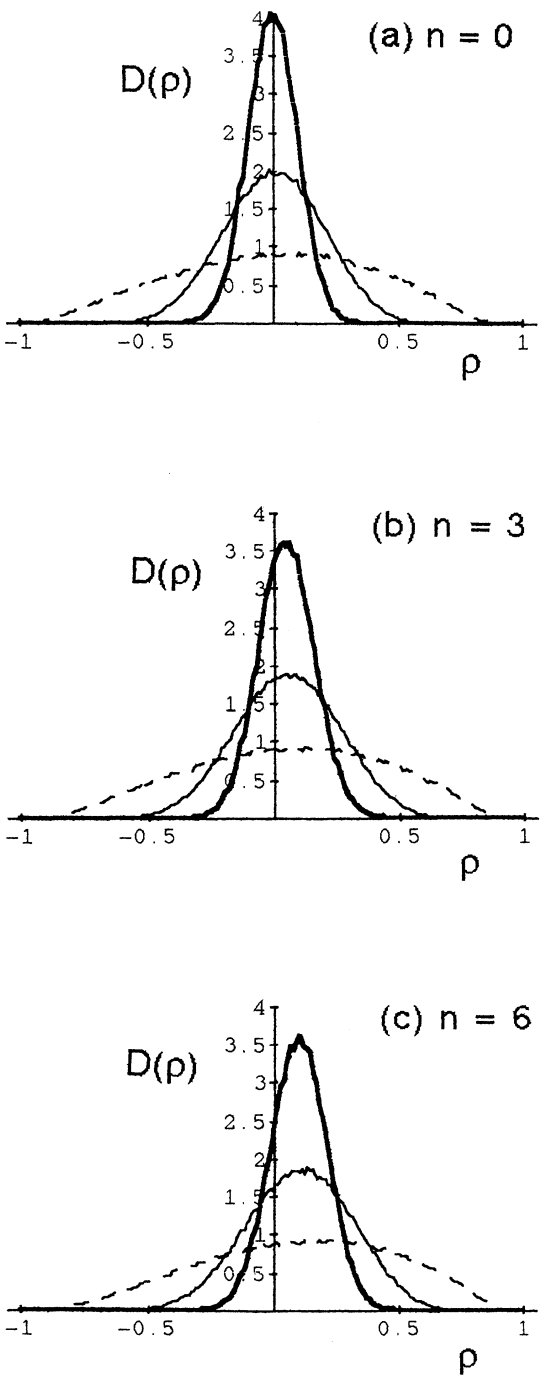

FIG. 6. Distribution function $D(\rho)$ of the excess electron density of the doped C_{60} in the presence of site disorders. The ordinate is normalized so that the area between the curve and the abscissa is unity. The thick, thin, and dashed lines are for $U_s=0.5$, 1.0, and 2.0 eV, respectively. ρ is in units of excess electron density.

VI. SUMMARY AND DISCUSSION

The effects on C_{60} of thermal fluctuations of phonons have been simulated by bond disorder potentials. Next, misalignment of C_{60} molecules in a crystal, and other intercalated impurities (C_{70}, oxygen atoms, dopants, and so on) have been studied with site disorder potentials. The extended SSH model for doped C_{60} has been solved with the assumption of the adiabatic approximation. The distributions of bond lengths and electron densities, $D(y)$ and $D(\rho)$, have been shown as functions of the disorder strength and the additional electron number. The stability of polaron excitations as well as dimerization patterns have been considered.

Our conclusions are common to bond and site disorder effects. Polarons and dimerizations in lightly doped cases ($C_{60}^{1-,2-}$) are relatively stable against disorders. This property has been indicated by peak structures in distribution functions. In more heavily doped cases, the several peaks merge into a single peak, showing the breakdown of polaron structures as well as the decrease of the dimerization strength.

However, there exist qualitative differences between bond and site disorder effects. In the bond disorder problem, the bond length is affected directly by the disorder potentials, but the charge density is modulated indirectly. In the site disorder problem, the charge density is modulated directly by the disorder potentials. Therefore, the distribution function of charge density shows the apparent peak structure related to the dimerization and polaronic distribution in the bond disorder problem, but it has only one peak in the site disorder problem.

Then how is our finding related with experiments? The NMR investigation[12] gives the evidence that there are two bond lengths in C_{60}. The single molecule always will be in the presence of some kinds of external potentials. These potentials could be effectively regarded as disorder. The presence of the two bond lengths in actual molecules agrees with our result that the dimerization is relatively stable against disorder. The ESR study[1] of the C_{60} monoanion in the solvent shows the reduced g factor. This is interpreted as the result of the Jahn-Teller distortion, in other words, the polaronic distortion. The molecules in the solvent would be affected by the strong site disorder as well as bond disorders. Nevertheless, the effect related to polarons is observed. This is again in accord with our conclusion that polarons are stable in light-

ly doped C_{60} in disordered external potentials.

The electrochemical experiment[15] can produce C_{60} anions doped with up to six electrons. The molecule can be doped with six electrons in the solid also. The photoemission experiments[2] show that the maximally doped C_{60} solid is an insulator. This agrees with the present calculation. However, it is not certain whether or not the dimerizations still remain in heavily doped C_{60}. In view of the fact that dimerizations are very small in heavily doped C_{60} and the width of zero-point motion of phonons is of the order of 0.01 Å,[11] it is certainly possible that the dimerization would not be observed in actual samples.

ACKNOWLEDGMENTS

Fruitful discussion with Professor G. A. Gehring, Dr. M. Fujita, and Dr. Y. Asai is acknowledged. Useful correspondences with Professor B. Friedman and Dr. S. Abe are also acknowledged. The author is grateful to Dr. M. Fujita for providing him with Figs. 1 and 2 of this paper.[16] Numerical calculations have been performed on FACOM M-1800/30 of the Research Information Processing System, Agency of Industrial Science and Technology, Japan.

*Electronic mail address: harigaya@etl.go.jp.
†Permanent address.

[1]T. Kato, T. Kodama, M. Oyama, S. Okazaki, T. Shida, T. Nakagawa, Y. Matsui, S. Suzuki, H. Shiromaru, K. Yamauchi, and Y. Achiba, Chem. Phys. Lett. **180**, 446 (1991).

[2]T. Takahashi, S. Suzuki, T. Morikawa, H. Katayama-Yoshida, S. Hasegawa, H. Inokuchi, K. Seki, K. Kikuchi, S. Suzuki, K. Ikemoto, and Y. Achiba, Phys. Rev. Lett. **68**, 1232 (1992); C. T. Chen, L. H. Tjeng, P. Rudolf, G. Meigs, L. E. Rowe, J. Chen, J. P. McCauley, Jr., A. B. Smith III, A. R. McGhie, W. J. Romanow, and E. W. Plummer, Nature (London) **352**, 603 (1991).

[3]S. Morita, A. A. Zakhidov, and K. Yoshino, Solid State Commun. **82**, 249 (1992); S. Morita, A. A. Zakhidov, T. Kawai, H. Araki, and K. Yoshino, Jpn. J. Appl. Phys. **31**, L890 (1992).

[4]M. Matus, H. Kuzmany, and E. Sohmen, Phys. Rev. Lett. **68**, 2822 (1992).

[5]P. A. Lane, L. S. Swanson, Q. X. Ni, J. Shinar, J. P. Engel, T. J. Barton, and L. Jones, Phys. Rev. Lett. **68**, 887 (1992).

[6]F. C. Zhang, M. Ogata, and T. M. Rice, Phys. Rev. Lett. **67**, 3452 (1991).

[7]K. Harigaya, J. Phys. Soc. Jpn. **60**, 4001 (1991); B. Friedman, Phys. Rev. B **45**, 1454 (1992).

[8]A. P. Su, J. R. Schrieffer, and A. J. Heeger, Phys. Rev. B **22**, 2099 (1980).

[9]K. Harigaya, Phys. Rev. B **45**, 13 676 (1992).

[10]McKenzie and Wilkins, Phys. Rev. Lett. **69**, 1085 (1992).

[11]B. Friedman and K. Harigaya, Phys. Rev. B **47**, 3975 (1993).

[12]C. S. Yannoni, P. P. Bernier, D. S. Bethune, G. Meijer, and J. R. Salem, J. Am. Chem. Soc. **113**, 3190 (1991).

[13]T. Arai, Y. Murakami, H. Suematsu, K. Kikuchi, Y. Achiba, and I. Ikemoto, Solid State Commun. **84**, 827 (1992).

[14]K. Harigaya (unpublished).

[15]Q. Xie, E. Pérez-Cordero, and L. Echegoyen, J. Am. Chem. Soc. **114**, 3978 (1992).

[16]The figures have been drawn by using the projection method on the honeycomb lattice, developed in M. Fujita *et al.*, Phys. Rev. B **45**, 13 834 (1992). This method can be applied to higher fullerenes for an understanding of dimerization patterns by bearing in mind relations with dimerizations on the honeycomb lattice.